1
2
3
4 **Superior discrimination for hue than for saturation; and an explanation in terms**
5 **of correlated neural noise.**
6
7 M. V. Danilova[1,2] and J. D. Mollon[2]
8

9 [1]Laboratory of Visual Physiology, I.P. Pavlov Institute of Physiology, Nab. Makarova 6, St.
10 Petersburg 199034 Russia
11
12 [2]Department of Psychology, Downing St., Cambridge CB2 3EB, United Kingdom

13
14 Keywords: Colour vision; colour discrimination; hue; saturation; correlated neural
15 noise.
16

17 Corresponding author: Dr. M. V. Danilova, mvd1000@cam.ac.uk

18
19
20 **Abstract**
21

22 The precision of human colour discrimination depends on the region of colour space in
23 which measurements are made and on the direction in which the compared colours –
24 the discriminanda – differ. Working in a MacLeod-Boynton chromaticity diagram scaled
25 so that thresholds at the white point were equal for the two axes, we made
26 measurements at reference points lying on lines that passed at 45° or -45° through the
27 white point. At a given reference chromaticity, we measured thresholds either for
28 *saturation* (i.e. for discriminanda lying radially along the line passing through the white
29 point) or for *hue* (i.e. for discriminanda lying on a tangent of a circle passing through the
30 reference point and centred on the white point). The discriminanda always straddled
31 the reference point in chromaticity. The attraction of this arrangement is that the two
32 thresholds can be expressed in common units: all that differs between saturation and
33 hue measurements is the phase with which the short-wave signal is combined with the
34 long-/middle-wave signal. Except for chromaticities very close to the white point,
35 saturation thresholds were systematically higher than hue thresholds. We offer a
36 possible explanation in terms of correlated neural noise.
37

1. Introduction

In the normal human retina, there are three classes of cone, maximally sensitive in different spectral regions [1]; and our perception of colour depends on neural comparisons of the rates at which photons are absorbed in the different classes [2]. Given three univariant signals, and thus two independent ratios, all visible colours can be represented on a two-dimensional surface. An example of such a 'chromaticity diagram' is the MacLeod-Boynton diagram (Fig. 1), whose ordinates are $L/(L+M)$ and $S/(L+M)$, where L,M,S are the excitations of the long-, middle- and short-wave cones respectively [3]. The two ordinates of this diagram have physiological counterparts: they correspond to the signals extracted by retinal ganglion cells of the *midget* and the *small bistratified* types [2].

Although a chromaticity diagram represents all colours, such diagrams do not accurately predict the discriminability of pairs of colours: a pair of chromaticities separated by a given geometrical distance in the diagram may or may not have the same discriminability as a second pair separated by the same distance, depending on the region of the diagram in which the paired chromaticities lie, the direction in which the individual chromaticities differ, and the state of adaptation of the eye [3-6]. Yet in many civil and commercial domains, it is important to be able to predict when two samples will be noticeably different in colour; and several linear and non-linear transformations of the CIE$_{(1931)}$ chromaticity diagram have been introduced, in successive attempts to achieve a 'uniform colour space' in which pairs of colours that are equally discriminable are separated by equal distances [7, 8].

(a) The super-importance of hue differences and the problem of Mongean noise.

In the present study, we compare two fundamental subtypes of colour discrimination: discrimination of saturation and discrimination of hue. We define the two types of threshold in terms of the geometry of the chromaticity diagram and not in terms of subjective appearances (so we neglect the Abney effect [9]). We define the white point in the diagram as the chromaticity of the neutral illumination to which the eye is currently adapted (here metameric to Daylight Illuminant D65). A pair of lights that differ in saturation are lights that lie along a line radiating from the white point. A circular set of chromaticities centred on the white point are described as varying in hue (see Fig. 1A) and the hue thresholds measured here are along tangents to such a circle.

[Figure 1 here]

Rather little known in the modern literature on visual science, but much discussed in the mid-twentieth century by those concerned with practical tolerances for surface colours, is a phenomenon that Judd called the 'super-importance of hue differences' [7, 8, 10]. Colour differences measured along a radial line in colour space – i.e. saturation differences – are smaller than would be expected from differences in an orthogonal direction, i.e. hue differences. If we construct a circle in colour space that is centred on the white point and has a radius of n units of perceptual distance, then it is found that the circumference – a hue circle – does not have $2\pi n$ units of perceptual distance but more like $4\pi n$ units. Judd concluded that there was no possible Euclidean representation of colour space in which equal distances corresponded to equal discriminability [10].

Judd was primarily concerned with supra-threshold differences, but there is some indication that the super-importance of hue also applies at threshold [11]. It is curious

89   that hue thresholds should be lower than saturation thresholds in this way. The neural
90   channels that extract chromatic information at early stages of the visual system are
91   usually thought of as signalling saturation: the channel is in equilibrium at the adapting
92   chromaticity and it signals departures from this neutral state [12]. Thus, in a
93   conventional view there might be four classes of units in the lateral geniculate nucleus,
94   signalling either increments or decrements along the two cardinal axes of chromaticity
95   space (Fig. 1B) [13]. To derive precise estimates of hues at angles between the cardinal
96   axes, some form of comparator would be required more centrally to extract the ratios of
97   the saturation signals generated in the distal channels. Estimates of saturation would
98   depend on the vector sum of the same signals and so it is not obvious why
99   psychophysical thresholds for hue should be substantially lower than those for
100   saturation. Below we offer a possible explanation of this paradox.
101
102   The classical evidence for the super-importance of hue differences was largely derived
103   from the viewing of surface colours, typically Munsell samples. Here there is the
104   possibility that physical noise contributes to any difference in discrimination. Real-
105   world surfaces reflect to the eye a specular component (representing the illuminant) as
106   well as a component (the body colour) that derives from selective absorption by
107   pigment molecules within the material. This was first made explicit by Gaspard Monge
108   in 1789 [14, 15]; and in modern accounts of colour constancy [16, 17] it has been
109   identified as a way in which the visual system could recover the chromaticity of the
110   illuminant by what could be called 'chromatic triangulation'. Even a matte surface is
111   represented not by a point in chromaticity space but by a distribution of chromaticities
112   that extends from the body colour towards the chromaticity of the illuminant.
113   Moreover, this variation will increase if eye position is not fixed and changes occur in
114   the angle of viewing the surface. We suggest the term 'Mongean noise' for this strictly
115   physical noise. Since Mongean noise lies on a radial line in chromaticity space, it should
116   raise thresholds for saturation but not for hue. It thus could contribute to the 'super-
117   importance of hue' when discrimination is measured with material surfaces.
118
119   **(b) The present measurements**. In the work reported here, we use a self-luminous
120   CRT display to compare hue discrimination and saturation discrimination while
121   avoiding the problem of Mongean noise. We measure thresholds for hue and for
122   saturation at reference chromaticities that lie on +45° and -45° radial lines passing
123   through the white point in the MacLeod-Boynton diagram (Fig. 1A, B). Saturation
124   measurements are made radially through the reference chromaticity and hue
125   measurements orthogonally through the same point. For each line, in each quadrant of
126   the diagram, we make measurements at different distances from the neutral point.
127
128   An essential requirement is a common metric for expressing the two types of threshold.
129   The salient feature of our design is that – for any given reference chromaticity – the
130   same modulation of the S-cone signal is combined with the same modulation of the
131    $L/(L+M)$ signal, but in different phases for saturation and for hue. Thus, in the upper
132   right quadrant of the MacLeod-Boynton diagram (Q1), saturation is measured when an
133   increment in $S/(L+M)$ is paired with an increment in $L/(L+M)$ and hue is measured by
134   pairing an increment in $S/(L+M)$ with a decrement in $L/(L+M)$. The target and distractor
135   stimuli always lay symmetrically on opposite sides of the reference stimulus: the target
136   always incorporated an increment in the $S/(L+M)$ signal and the distractors
137   incorporated a decrement in $S/(L+M)$.
138

139 The scaling of the vertical axis of a MacLeod-Boynton diagram is arbitrary [18] and the
140 angle taken as 45° will depend on this scaling. We followed recent tradition in the study
141 of chromatic discrimination [19, 20] and scaled the $S/(L+M)$ ordinate so that thresholds
142 for excursions around the white point were equal for the two cardinal axes. Thus when
143 below we refer to hue thresholds we formally mean thresholds measured along a line
144 orthogonal to a radial line at 45° or -45° in the scaled space (Fig. 1).
145
146 In classical studies of colour discrimination, the observer was often able to inspect the
147 surfaces or lights for an extended period before making a judgement [e.g. 11, 21], and
148 this would allow the chromatic channels of the visual system to adapt towards the
149 current chromaticity – 'self-adaptation' to the target stimulus. Thus measurements in
150 different parts of chromaticity space might be made in different states of adaptation.
151 This would be appropriate for setting tolerances for real-world surfaces, where viewing
152 conditions would be similar; but it is inappropriate if the purpose is to analyse the visual
153 mechanisms of discrimination. In the present study, we set out to minimally perturb the
154 observer's adaptation: a neutral adapting field was continuously present and
155 discrimination was probed with a brief array of target and distractor stimuli.
156
157 **2. Materials and methods**
158 **(a) Observers**
159 The observers comprised the authors and three other, female, observers who were
160 highly practised but were naïve as to the purpose of the experiments. All had normal
161 colour vision as tested by the Cambridge Colour Test [22]. All observers gave informed
162 consent according to Declaration of Helsinki.
163
164 **(b) Apparatus and stimuli**
165 Two of the observers were tested in St Petersburg (Russia), three in Cambridge (UK)
166 using the same experimental programs. In both laboratories, stimuli were presented on
167 calibrated Mitsubishi CRT monitors (Diamond Pro 2070), controlled by Cambridge
168 Research Systems (CRS) graphics systems (Visage in St Petersburg, VSG 2/3 in
169 Cambridge,). For calibration procedures and monitor settings, see ref [23].
170
171 The monitor was viewed binocularly from 57 cm. The steady white background field
172 had a luminance of 10 cd.m^{-2} and its chromaticity was that of Illuminant D65 [6]. A
173 diamond array of black points guided fixation.   The stimulus array was presented to the
174 fovea and consisted of a disc divided into 4 sectors (inset, Fig. 1B). One sector, chosen at
175 random on each presentation, was the target (T) and the remaining sectors were
176 distractors (D). The array subtended 2 degrees of visual angle.
177
178 The duration of the array was 200 ms. This value is a compromise between the self-
179 adaptation that may occur at long exposures (see above) and the 'tachistoscopic
180 tritanopia' known to affect very brief presentations [24]. In preliminary measurements
181 along the two cardinal axes at the white point, we observed tachistoscopic tritanopia
182 below 200 ms, in that that the ratio of $S/(L+M)$ thresholds to $L/(L+M)$ thresholds
183 increased markedly. The ratio was relatively stable for durations >200 ms.
184
185 We specified chromaticities in a MacLeod-Boynton diagram constructed from the cone
186 sensitivities of DeMarco and colleagues [25]. The diagram represents a plane of equal
187 luminance for the Judd$_{1951}$ Observer, where luminance equals the sum of L- and M-cone
188 signals [26]. We scaled the vertical ordinate so that thresholds for departures from the
189 white point were equal on the two cardinal axes. In these preliminary measurements,

190   we used the same configuration, duration and procedures as for the main experiments,
191   and obtained thresholds for increments and decrements from the white point along the
192   two axes for three of our observers. For each observer there were 5 independent
193   estimates of each threshold. On the basis of the average thresholds, we adopted the
194   scaling factor 1.7054 relative to the ordinate of the classical MacLeod-Boynton diagram
195   [27]. As a check, we repeated the measurements after scaling, obtaining a ratio of 1.02
196   (SEM: 0.04) between thresholds on the two axes.

197

198   The test array had an average luminance 30% greater than that of the background when
199   expressed in the $L+M$ units of our space; but to ensure that observers could not
200   discriminate the target from the distractors by differences in sensation luminance, we
201   jittered independently the $L+M$ value of each sector by ±1%.

202

203   **(c) Procedure**
204   Thresholds were measured along four lines radial to the chromaticity of D65 and at
205   angles of either 45° or -45° (Fig. 1B). Along each line, measurements were centred on a
206   reference chromaticity that differed from D65 in $L/(L+M)$ value by 1%, 2% or 3%. In the
207   orange and green regions, a 3% shift in $L/(L+M)$ brings the measurements close to the
208   monitor gamut.

209

210   On any trial, the observer made a spatial forced choice, indicating by pushbuttons which
211   sector of the test array differed in chromaticity from the remaining three. Auditory
212   feedback was given. In any one experimental session, thresholds were measured for
213   reference stimuli at one distance from D65 on all four lines. Within the session, hue and
214   saturation thresholds at a given reference were measured in separate blocks of trials,
215   thus giving a total of 8 blocks in one session. The orders of blocks and of sessions were
216   randomised.

217

218   During each threshold measurement, the reference chromaticity was never itself
219   presented, but the discriminanda lay on a line passing through the reference and
220   straddling the reference value. The chromatic separation of the discriminanda was
221   increased or decreased symmetrically around the reference chromaticity according to
222   the observer's accuracy. The staircase procedure tracked 79.4% correct: see ref [23].
223   The staircase terminated after 15 reversals, the last 10 being averaged to give the
224   threshold. There were 6 sets of experimental runs, the first set being treated as practice.
225   Thus any given threshold for a given observer is based on 5 independent repetitions.

226

227   **3. Results**

228

229   [Figure 2 here]

230

231   In the bar chart of Fig. 2 we show illustrative data for an observer who was unaware of
232   the purpose of the experiments. The ordinate shows the difference (Δ) between the
233    $L/(L+M)$ coordinates of the target and distractors (since measurements are made at 45°,
234   the difference in $S/(L+M)$ is identical; see Methods). Each panel corresponds to
235   measurements made at different distances from D65; and within each panel each pair of
236   thresholds corresponds to one quadrant of the MacLeod-Boynton diagram (See Fig 1B
237   for the numbering of quadrants). In all but one case, the threshold for hue is lower than
238   the threshold for saturation measured at the same reference chromaticity. The absolute
239   size of the thresholds increases with distance from the adapting chromaticity, i.e. as one

240　passes from the first to the third panel. And Q1 (the upper right quadrant) shows the
241　weakest difference between hue and saturation.
242
243　　　　　　　　　　　　　　　　[Figure 3 here]
244
245　Fig. 3 shows average results for all observers plotted directly in our scaled MacLeod-
246　Boynton diagram after the manner of W.D.Wright's dashes [28]: the lengths of the line
247　segments represent the separation of the discriminanda needed to sustain a
248　performance of 79.4% correct. The pattern of results in general reflects that seen for an
249　individual observer in Fig. 2: saturation thresholds at a given reference chromaticity are
250　usually larger than for hue; the difference is least marked in Q1; and the absolute sizes of
251　all thresholds increase with distance of the reference chromaticity from the white point.
252　The latter is a classical finding [e.g. 19, 20, 29-33]. A repeated measures ANOVA with
253　factors Hue vs. Saturation, Distance from D65 and Quadrant, shows (after Greenhouse-
254　Geisser correction) significant effects of Hue vs. Saturation ($F[1,4]=60.8$, $p<0.001$),
255　Distance from D65 ($F[1.22,4.92]=46.1$, $p<0.001$) and Quadrant ($F[1.67,6.66]=12.7$,
256　$p=0.006$). There was a highly significant interaction between Hue vs. Saturation and
257　Distance from D65 ($F[1.64,6.57]=29.1$, $p<0.001$) and a marginally significant interaction
258　between Distance from D65 and Quadrant ($F[1.5,6]=6.2$, $p=0.04$.
259
260　　　　　　　　　　　　　　　　[Figure 4 here]
261
262　In Fig. 4 we plot ratios of saturation thresholds to hue thresholds for the separate
263　quadrants of the MacLeod-Boynton diagram. All quadrants show an increasing ratio
264　with increasing distance from the white point, but systematic differences between
265　quadrants are apparent. The superiority of hue discrimination is most marked in Q4
266　(upper left) and least marked in Q1. However, the latter quadrant shows the strongest
267　change in ratio.
268
269　**4. Control experiment: effects of luminance jitter.**
270
271　In our main experiment, we introduced a ±1% luminance jitter to ensure that observers
272　used only chromatic cues. This was a conservative precaution, since chromatic
273　discrimination typically surpasses luminance discrimination [e.g. 34], and the small gaps
274　between our fields would favour chromatic rather than luminance discrimination [35].
275　Is it possible, nevertheless, that the luminance jitter elevated saturation thresholds
276　disproportionately? We performed a control experiment in which different levels of
277　jitter (0%, 1%, 3% and 5%) were introduced in different blocks of trials. The observers
278　and procedures were otherwise as for the main experiment, except that we tested at
279　only one distance from the white point (2%).
280
281　　　　　　　　　　　　　　　　[Figure 5 here]
282
283　Results for this control experiment are shown in Fig. 5. The four panels, corresponding
284　to the four quadrants, are inset at their appropriate positions within the MacLeod-
285　Boynton diagram. The ordinates of the inset panels show the distance between the
286　discriminanda at threshold. It is clear that the superiority of hue discrimination
287　survives when no jitter is present and that increasing jitter has similar effects on the two
288　types of threshold. A repeated-measures ANOVA shows (after Greenhouse-Geisser
289　correction) significant effects of Hue vs. Saturation ($F[1,4]=71.1$, $p<0.001$), Jitter

290   (F[1.64,6.57] = 29.3, p<0.001) and Quadrant (F[2.54,10.17] = 12.3, p<0.001). There
291   were no significant interactions.
292
293   **5. Hue and saturation thresholds very close to the white point**
294
295   Fig. 4 suggests that the ratio between the two types of threshold grows with distance
296   from the white point. For three observers we have made supplementary measurements
297   very close to the white point, at reference chromaticities that differ from the *L/(L+M)*
298   value of D65 by 0.1%, 0.25%, 0.6% and 1%. The reference chromaticities lay on +45°
299   and -45° lines as before and the other experimental procedures were as for the main
300   experiment.
301
302   [Figure 6 here]
303
304   Fig. 6 shows results for this supplementary experiment. For quadrants 2 and 4 of the
305   diagram, hue discrimination is superior even at the smallest distance from the white
306   point; but for the remaining two quadrants the effect is attenuated or reversed. A
307   repeated-measures ANOVA showed, as might be expected from Fig. 6, no significant
308   effect of Hue vs Saturation, of Distance from D65 or of Quadrant, but (after Greenhouse-
309   Giesser correction) significant interactions between Hue vs Saturation and Quadrant
310   (F[1.07,2.15]=30.49, p=0.027) and Hue vs Saturation and Distance from D65
311   (F[1.93,3.85]=18.65, p=0.011).
312
313   **6. Discussion**
314
315   **(a) The superiority of hue discrimination. An hypothesis in terms of correlated**
316   **neural noise.**
317
318   Our main experiment reveals a general superiority for hue discrimination relative to
319   discrimination of saturation.   The experimental conditions ensured that the two types of
320   measurement differed only in the signs with which modulations on the cardinal axes
321   were combined, and the modulations were always centred on the same reference
322   chromaticity. So the magnitudes of the two types of thresholds can be directly
323   compared. Clearly it would not be possible, from threshold measurements made under
324   the present conditions, to construct a Euclidean colour space in which equal geometric
325   distances corresponded to equal discriminability (see Introduction).
326
327   Why should thresholds for saturation systematically exceed those for hue? We offer a
328   provisional theory in terms of correlated neural noise within the visual system.
329
330   In both the retina and the visual cortex, neurons are known to exhibit correlated
331   variations in excitability [36-38]. Typically, the correlations are attenuated with
332   increasing spatial separation of a given pair of neurons. Of especial interest for our
333   present study is the demonstration by Greschner and colleagues of correlation in the
334   primate retina between neural firing in small bistratified ganglion cells (which draw ON
335   input from S cones) and that in nearby ON midget cells (which draw ON input from
336   either L or M cones) [38].
337
338   [Figure 7 here]
339

8

340   Fig. 7 illustrates our hypothesis of how correlated neural noise might lead to superior
341   hue discrimination. The axes of each panel represent the neural signals in the two
342   chromatic channels of the early visual system. In each panel, T indicates the target and
343   D the distractors in our forced-choice experiment. The left-hand panels represent the
344   case of hue discrimination and the right-hand panels represent the case of saturation.
345   The geometrical distance between T and D is equal in left and right panels.
346
347   The upper panels (a) represent the case where there is no noise in the neural signals:
348   the target and the distractors then plot as points. The middle panels (b) represent the
349   case where independent, uncorrelated, gaussian noise is present in the two neural
350   channels. Each circle represents one contour of the probability density distribution of
351   the neural responses produced by a given chromaticity. The lowermost panels (c)
352   represent the case where the noise in the two channels is correlated. Now the
353   probability density distributions are elliptical, since fluctuations in the two channels co-
354   vary.   The distributions overlap in the case of saturation shifts but not in that of hue
355   shifts. For the cardinal signals are combined with different signs in the two cases. In the
356   case of hue, the $S/(L+M)$ signal is higher for the target and lower for the distractors,
357   whereas the opposite is true for the $L/(L+M)$ signal. In the case of saturation, however,
358   both the $S/(L+M)$ signal and the $L/(L+M)$ signal are higher for the target and lower for
359   the distractors. Since the correlated neural noise causes the two probability density
360   distributions to overlap, discrimination will be poorer for saturation.
361
362   The 'super-importance of hue' has sometimes led to the conclusion that hue and
363   saturation are analysed by different systems. This view was classically expressed by
364   Kuehni, who wrote 'In practical terms, there appear to be two independent systems:
365   one that assesses changes in the ratio of two opponent color signals (assuming a two-
366   process hue detection system) and the other changes in the size of the vector sum of the
367   opponent color system (indicative of contrast)…The two seemingly operate
368   independently of each other and are not connected in a euclidean sense.' [8 ch 8]. Our
369   hypothesis suggests how the two types of discrimination might depend on the same
370   distal signals – although necessarily in one case it is the ratio of those signals that is
371   identified and in the other, it is their sum.
372
373   An interesting analogy can be made between hue and saturation, on the one hand, and
374   the auditory attributes of pitch and loudness on the other. In the classification of S. S.
375   Stevens, hue is a *metathetic* sensory dimension like pitch, and saturation is *prothetic* like
376   loudness [39]. In psychoacoustics it has often been held that frequency discrimination
377   could not depend on the same neural signals as intensity discrimination. The latter is
378   thought to depend on the spike rate of cortical neurons, but the relatively high
379   resolution observed for frequency suggested that pitch discrimination could not depend
380   on the same signal and instead must depend on the timing of spikes. However, Micheyl
381   and colleagues [40] explain the disparity of the two types of threshold by correlated
382   noise in the same types of neuron.
383
384   In the case of vision, a hypothesis analogous to the present one was explored by Regan
385   and Beverley for the case of orientation discrimination [41 p 153]. They point out the
386   general principle that 'Opponent processing has the feature that noise in the first-stage
387   outputs…can be partially or even completely suppressed by the opponent element.'
388
389   **(b) Intermediate colour channels?**
390

391　For the purposes of the model outlined above, we took the primary signals to be
392　*S/(L+M)* and *L/(L+M),* but chromatic channels tuned to intermediate, non-cardinal,
393　directions of colour space have often been postulated [see e.g. 42] – channels that are
394　usually taken to be central to the 'cardinal' channels but could conceivably be in parallel
395　with them [43]. In principle, an explanation of the type offered above could still apply if
396　hue discrimination depended on a comparison of the signals in channels tuned to
397　intermediate directions in colour space.
398
399　Discrimination ellipses oriented obliquely have actually been taken as independent
400　evidence for 'intermediate' chromatic channels. Our hypothesis of correlated noise
401　offers an alternative explanation for such ellipses.
402
403　**(c) Variation between quadrants of the MacLeod-Boynton diagram**
404
405　For reference chromaticities at moderate distances from the white point, it appears to
406　be a general rule that saturation thresholds exceed those for hue; and above we offered
407　a possible explanation for this result. However, a complete explanation will need to take
408　into account the differences of the strength of the effect in different quadrants of the
409　MacLeod-Boynton diagram (Fig. 4). For Q2 (lower right) and Q4 (upper left), the ratios
410　are largest, and the effect is maintained in regions very close to the white point (Fig. 6),
411　whereas the effect is attenuated or reversed near the white point for quadrants 1 and 3.
412　These results are consistent with earlier studies [19, 20] where discrimination ellipses
413　were measured in the different quadrants of DKL [13] space. And a similar pattern is
414　seen in the variance of thresholds for different observers in the results of Elliott, Werner
415　and Webster [42].
416
417　In this context, we note a provocative coincidence. In the present experiment, in
418　equating cardinal axes to give equal thresholds at the white point, we found that we
419　needed to scale the *S/(L+M)* ordinate of the MacLeod-Boynton diagram by a factor of
420　~1.71. Independently, in earlier experiments [43], we scaled this ordinate so that a line
421　running between the wavelengths of unique yellow and unique blue ran at -45°: a very
422　similar factor (1.64) was needed. The locus of unique yellows and blues in turn closely
423　coincides with the 'caerulean line' in the outside world – the locus comprising mixtures
424　of skylight and sunlight [15, 44].
425
426　This means that in quadrants 2 and 4, the present saturation thresholds lie
427　approximately along the locus of unique yellows and blues, while hue judgements in
428　these quadrants coincide with the category boundary between reddish and greenish
429　hues. We have earlier noted that an optimum of discrimination occurs in the latter case
430　[43, 45], i.e. where thresholds are being measured orthogonally to the unique-blue locus.
431　It remains possible that this region of enhanced discrimination does correspond to the
432　equilibrium point of a intermediate neural channel that draws opposed inputs from M
433　cones and from L + S cones (For discussion, see ref [43].)
434
435　**7. Conclusions**
436　Within the area of colour space that we have explored, thresholds for discriminating
437　saturation are systematically higher than those for discriminating hue, except for
438　chromaticities very close to the white point. We offer a possible explanation in terms of
439　correlated neural noise in distal chromatic channels in the visual system. There is
440　empirical evidence that noise in these two channels is indeed correlated [38].
441

442   The experiments in both Cambridge and St. Petersburg were approved by the
443   Psychology Research Ethics Committee of the University of Cambridge.
444
445   **Acknowledgement.**   We thank Sungmi Oh, the referees and the editors for valuable
446   discussion.
447
448   **Data accessibility**: Dryad doi:10.5061/dryad.76gg2.
449
450   **Authors' contributions**. The authors contributed equally to the design and conduct of
451   the experiments and to the preparation of the manuscript.
452
453   **Figure legends**
454
455   1A. The distinction between thresholds for saturation and for hue shown in a portion of
456   the MacLeod-Boynton chromaticity diagram. B. A section of the MacLeod-Boynton
457   diagram showing the reference stimuli used in our main experiment. 'R,G,B' indicate the
458   chromaticities of the individual guns of our CRT monitor; and the solid triangle
459   connecting these points shows the gamut of available chromaticities. 'Q1, Q2, Q3, Q4'
460   indicate our numbering of the four quadrants of the diagram. 'D65' indicates the white
461   point, metameric to Illuminant D65. The dotted line at the bottom of the diagram
462   indicates part of the spectrum locus. Inset: spatial configuration of the stimulus array.
463
464   2. Results for an individual observer. The three panels show thresholds measured at
465   three different distances from the white point. Within each panel, pairs of threshold
466   (saturation and hue) are shown for the four quadrants of the MacLeod-Boynton diagram,
467   numbered as in Fig 1B. Thresholds are expressed as the difference (Δ) in $L/(L+M)$
468   coordinate between target and distractors. Error bars show ± 1 SEM and are based on
469   the variance of 5 independent measures of each threshold.
470
471   3. Average results for 5 observers, plotted in the MacLeod-Boynton diagram.   The
472   dashes directly show the separation of targets and distractors at threshold. 'D65'
473   indicates the chromaticity of the neutral adapting field. The dotted line indicates part of
474   the spectrum locus.
475
476   4. Ratios of saturation and hue thresholds.   Ratios are shown separately for each
477   quadrant of the MacLeod-Boynton diagram (numbered as in Fig. 1B).
478
479   5. Average thresholds for hue (triangles) and for saturation (circles) as a function of
480   luminance jitter. The 4 sets of data are symbolically placed within the appropriate
481   quadrants of the MacLeod-Boynton diagram. These measurements were all made at
482   reference chromaticities that differed from D65 by 2% in their L/(L+M) coordinate.
483   Error bars show ± 1 SEM and are based on the inter-observer variance.
484
485   6. Supplementary measurements of hue and saturation thresholds very close to the
486   white point. The abscissa of each panel shows the distance from the white point
487   expressed as the percentage change in the $L/(L+M)$ coordinate at the reference
488   chromaticity at which the two types of threshold were measured. The 4 sets of data are
489   symbolically placed within the appropriate quadrants of the MacLeod-Boynton diagram.
490   Error bars show ± 1 SEM.
491

492   7. How correlated neural noise could explain the superiority of hue discrimination. In
493   each panel the x and y axes represent the signals in the two 'cardinal' chromatic
494   channels of the early visual system.   The left-hand panels correspond to hue
495   discrimination and those to the right correspond to saturation discrimination. In the
496   upper panels (a), no noise is assumed: the responses generated by the target (T) and
497   the distractors (D) plot as points in the two-dimensional space. The middle panels (b)
498   correspond to the case where independent Gaussian noise is present in the two cardinal
499   channels. The circles represent one contour of the probability density function
500   produced by a given chromaticity. In the lowermost panels (c) it is assumed that noise
501   in the two channels is correlated. Now the probability density distributions are elliptical
502   with positive slopes. When the stimuli differ in saturation (right-hand panel) the
503   distributions for the discriminanda overlap; but when the stimuli differ in hue – when a
504   change on one axis is accompanied by an opposite change on the other axis – the overlap
505   of the probability density distributions is less.
506

References

1. Dartnall, H.J.A., J.K. Bowmaker, and J.D. Mollon, *Human visual pigments: microspectrophotometric results from the eyes of seven persons.* Proceedings of the Royal Society of London B, 1983. **220**: p. 115-130.

2. Dacey, D.M. and O.S. Packer, *Colour coding in the primate retina: diverse cell types and cone-specific circuitry.* Current Opinion in Neurobiology, 2003. **13**(4): p. 421-427.

3. MacLeod, D.I.A. and R.M. Boynton, *Rectangular chromaticity diagram showing cone excitations at constant luminance*, in *Colour Vision Deficiencies V*, G. Verriest, Editor. 1979, Adam Hilger: Bristol. p. 65-68.

4. Tyndall, E.P.T., *Chromaticity sensibility to wave-length difference as a function of purity.* Journal of the Optical Society of America, 1933. **23**: p. 15-24.

5. Le Grand, Y., *Les seuils différentiels de couleurs dans la théorie de Young.* Revue d'Optique théor. exp., 1949. **28**: p. 261-278.

6. Wyszecki, G. and W.S. Stiles, *Color Science.* 2nd ed. 1982, New York: Wiley.

7. Judd, D.B., *Ideal color space.* Color Engineering, 1970. **8**: p. 37-52.

8. Kuehni, R.G., *Color space and its divisions.* 2003, Hoboken, NJ: Wiley.

9. Burns, S.A., et al., *The Abney Effect: chromaticity coordinates of unique and other constant hues.* Vision Research, 1984. **24**: p. 479-489.

10. Judd, D.B., *Ideal color space: the super-importance of hue differences and its bearing on the geometry of color space.* Palette, 1969. **30**: p. 21-28.

11. Brennan, J.G. and S.M. Newhall, *ICI Specifications of Difference Limens for Munsell Hue, Value, and Chroma.* Journal of the Optical Society of America, 1948. **38**(8): p. 696-702.

12. DeValois, R.L. and R.T. Marrocco, *Single cell analysis of saturation discrimination in the macaque.* Vision Res, 1973. **13**(3): p. 701-11.

13. Derrington, A.M., J. Krauskopf, and P. Lennie, *Chromatic mechanisms in lateral geniculate nucleus of macaque.* Journal of Physiology, 1984. **357**: p. 241-65.

14. Monge, G., *Mémoire sur quelques phénomènes de la vision.* Annales de Chimie, 1789. **3**: p. 131-147.

15. Mollon, J.D., *Monge.* Visual Neuroscience, 2006. **23**: p. 297-309.

16. Lee, H.-C., *Method for computing the scene-illuminant chromaticity from specular highlights.* Journal of Optical Society of America, 1986. **A 3**: p. 1694-1699.

17. Hurlbert, A.C., *Computational models of colour constancy*, in *Perceptual Constancy: Why things look as they do.*, V. Walsh and J. Kulikowski, Editors. 1998, CUP: Cambridge.

18. Macleod, D.I.A. and R.M. Boynton, *Remarks on the Constant Luminance Chromaticity Diagram.* Color Research and Application, 1989. **14**(3): p. 157-158.

19. Krauskopf, J. and K. Gegenfurtner, *Color discrimination and adaptation.* Vision Research, 1992. **32**(11): p. 2165-75.

20. Sankeralli, M.J. and K.T. Mullen, *Ratio model for suprathreshold hue-increment detection.* Journal of the Optical Society of America a-Optics Image Science and Vision, 1999. **16**(11): p. 2625-2637.

21. MacAdam, D.L., *Visual sensitivities to color differences in daylight.* Journal of the Optical Society of America, 1942. **32**: p. 247-281.

22. Regan, B.C., J.P. Reffin, and J.D. Mollon, *Luminance noise and the rapid determination of discrimination ellipses in colour deficiency.* Vision Research, 1994. **34**: p. 1279-1299.

23. Danilova, M.V. and J.D. Mollon, *Is discrimination enhanced at the boundaries of perceptual categories? A negative case.* Proceedings of the Royal Society B-Biological Sciences, 2014. **281**(1785).

558   24.   Mollon, J.D., *A taxonomy of tritanopias*, in *Colour Vision Deficiencies VI*, G. Verriest,
559   Editor. 1982, Dr. W. Junk: The Hague. p. 87-101.
560   25.   DeMarco, P., J. Pokorny, and V.C. Smith, *Full-Spectrum Cone Sensitivity Functions*
561   *for X-Chromosome-Linked Anomalous Trichromats.* Journal of the Optical Society
562   of America A-Optics Image Science and Vision, 1992. **9**(9): p. 1465-1476.
563   26.   Smith, V.C. and J. Pokorny, *Spectral sensitivity of the foveal cone photopigments*
564   *between 400 and 500 nm.* Vision Research, 1975. **15**: p. 161-171.
565   27.   MacLeod, D.I.A. and R.M. Boynton, *Chromaticity diagram showing cone excitation*
566   *by stimuli of equal luminance.* Journal of the Optical Society of America, 1979. **69**:
567   p. 1183-1186.
568   28.   Wright, W.D., *The sensitivity of the eye to small colour differences.* Proceedings of
569   the Physical Society, 1941. **53**: p. 93-112.
570   29.   Schönfelder, W., *Der Einfluss des Umfeldes auf die Sicherheit der Einstellung von*
571   *Farbengleichungen.* Zeitschrift für Sinnesphysiologie, 1933. **63**: p. 228-251.
572   30.   Rautian, G.N. and V.P. Solov'eva, *Vlijanie svetlogo okrugenija na ostrotu*
573   *cvetorazlochenija.* Doklady Academii Nauk SSSR, 1954. **95**: p. 513-515.
574   31.   Loomis, J.M. and T. Berger, *Effects of chromatic adaptation on color discrimination*
575   *and color appearance.* Vision Research, 1979. **19**: p. 891-901.
576   32.   Miyahara, E., V.C. Smith, and J. Pokorny, *How Surrounds Affect Chromaticity*
577   *Discrimination.* Journal of the Optical Society of America a-Optics Image Science
578   and Vision, 1993. **10**(4): p. 545-553.
579   33.   Danilova, M.V. and J.D. Mollon, *Symmetries and asymmetries in chromatic*
580   *discrimination.* Journal of the Optical Society of America a-Optics Image Science
581   and Vision, 2014. **31**(4): p. A247-A253.
582   34.   Chaparro, A., et al., *Colour is what the eye sees best.* Nature, 1993. **361**: p. 348-350.
583   35.   Boynton, R.M., M.M. Hayhoe, and D.I.A. MacLeod, *The gap effect: chromatic and*
584   *achromatic visual discrimination as affected by field separation.* Optica Acta, 1977.
585   **24**: p. 159-177.
586   36.   Smith, M.A. and M.A. Sommer, *Spatial and Temporal Scales of Neuronal*
587   *Correlation in Visual Area V4.* Journal of Neuroscience, 2013. **33**(12): p. 5422-
588   5432.
589   37.   Lin, I.C., et al., *The Nature of Shared Cortical Variability.* Neuron, 2015. **87**(3): p.
590   644-656.
591   38.   Greschner, M., et al., *Correlated firing among major ganglion cell types in primate*
592   *retina.* Journal of Physiology-London, 2011. **589**(1): p. 75-86.
593   39.   Panek, D.W. and S.S. Stevens, *Saturation of Red - Prothetic Continuum.* Perception
594   & Psychophysics, 1966. **1**(2): p. 59-66.
595   40.   Micheyl, C., P.R. Schrater, and A.J. Oxenham, *Auditory Frequency and Intensity*
596   *Discrimination Explained Using a Cortical Population Rate Code.* Plos
597   Computational Biology, 2013. **9**(11).
598   41.   Regan, D. and K.I. Beverley, *Postadaptation Orientation Discrimination.* Journal of
599   the Optical Society of America a-Optics Image Science and Vision, 1985. **2**(2): p.
600   147-155.
601   42.   Elliott, S.L., J.S. Werner, and M.A. Webster, *Individual and age-related variation in*
602   *chromatic contrast adaptation.* J Vis, 2012. **12**(8).
603   43.   Danilova, M.V. and J.D. Mollon, *Foveal color perception: Minimal thresholds at a*
604   *boundary between perceptual categories.* Vision Research, 2012. **62**: p. 162-172.
605   44.   Mollon, J.D. and R.J. Lee, *Do unique hues originate within us or in the outside*
606   *world?* Perception, 2008. **37**: p. 127-127.
607   45.   Danilova, M.V. and J.D. Mollon, *Parafoveal color discrimination: a chromaticity*
608   *locus of enhanced discrimination.* Journal of Vision, 2010. **10**(1).
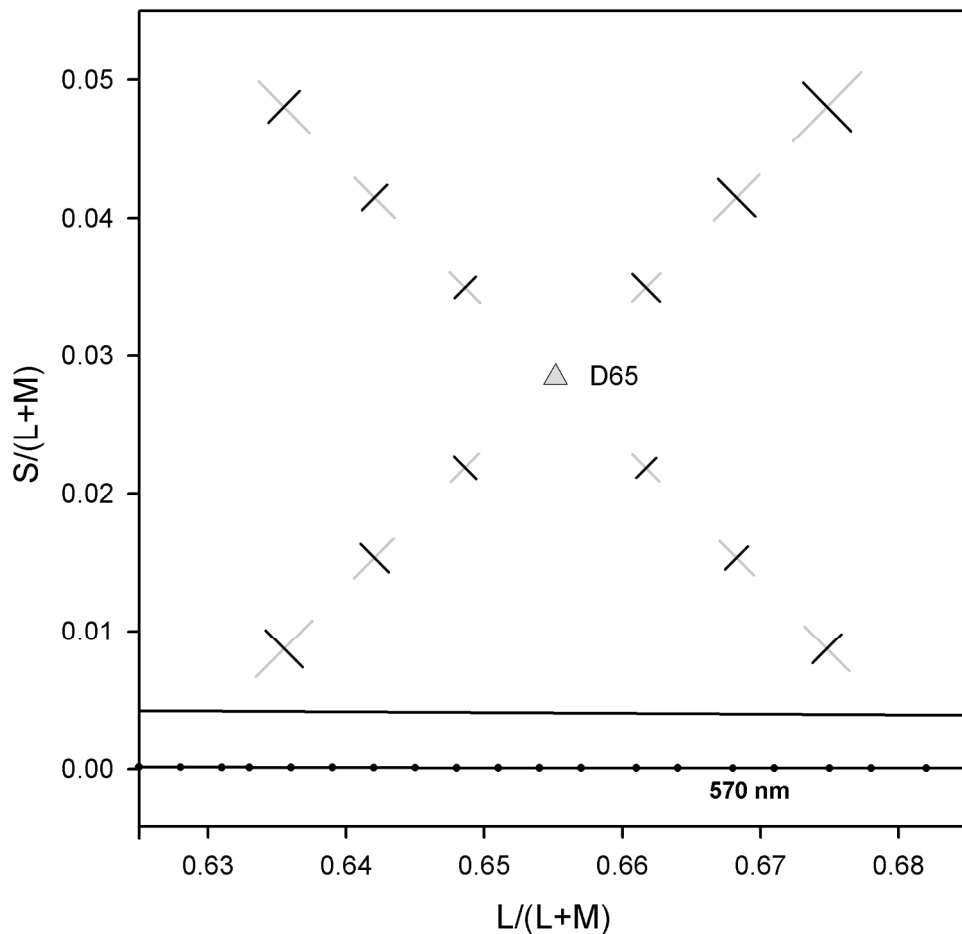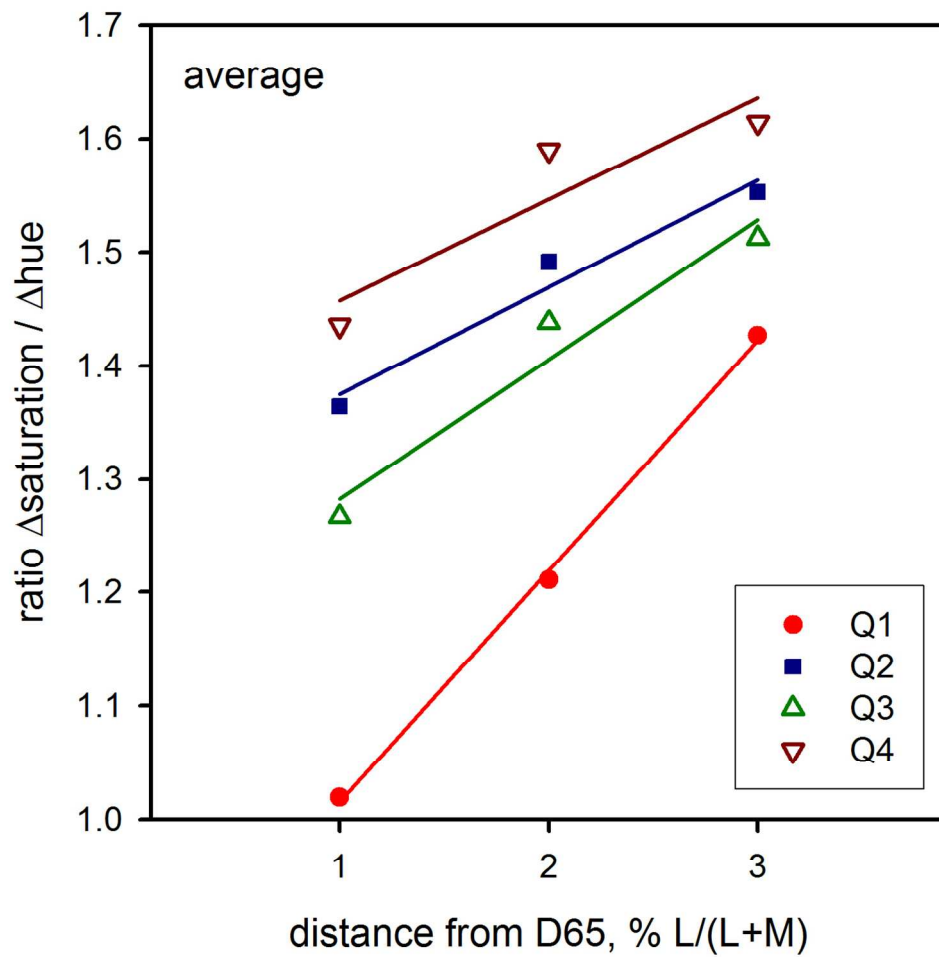
14

609
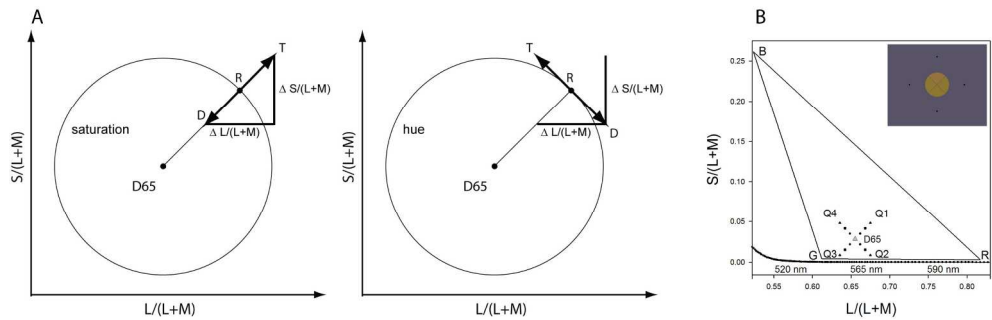
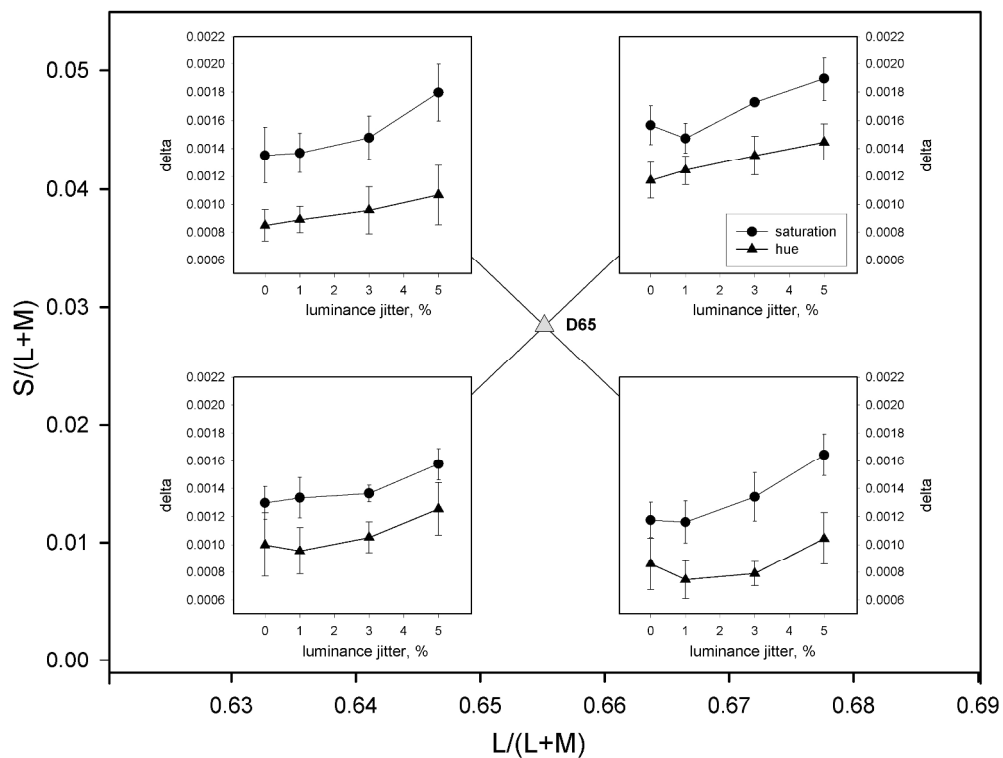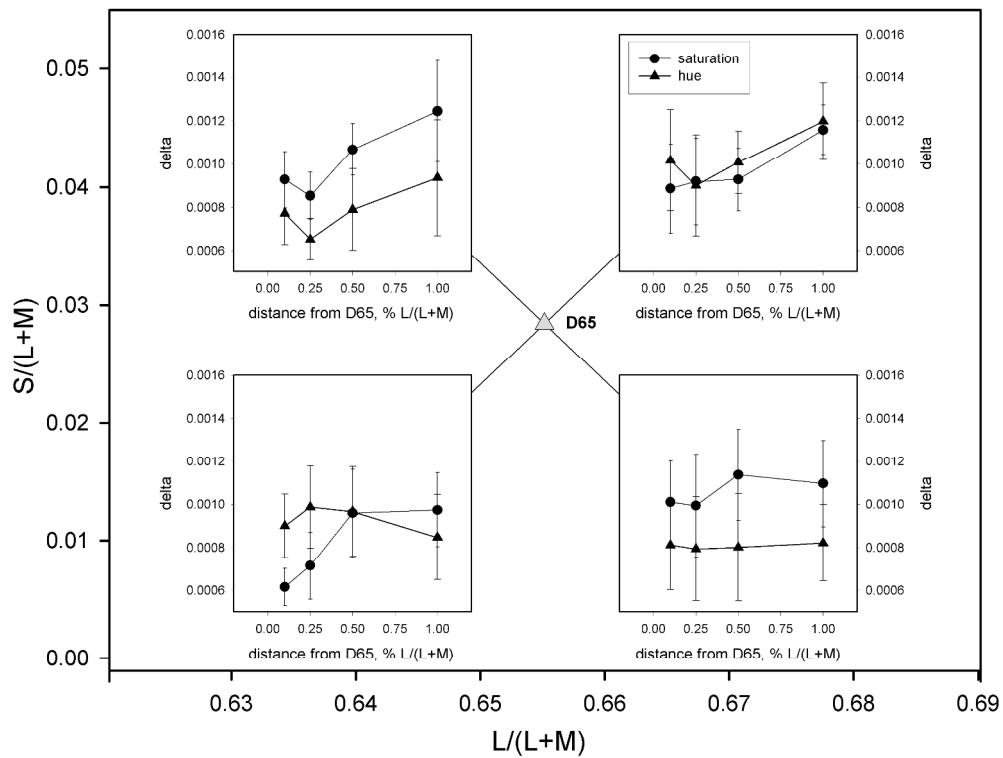208x66mm (300 x 300 DPI)
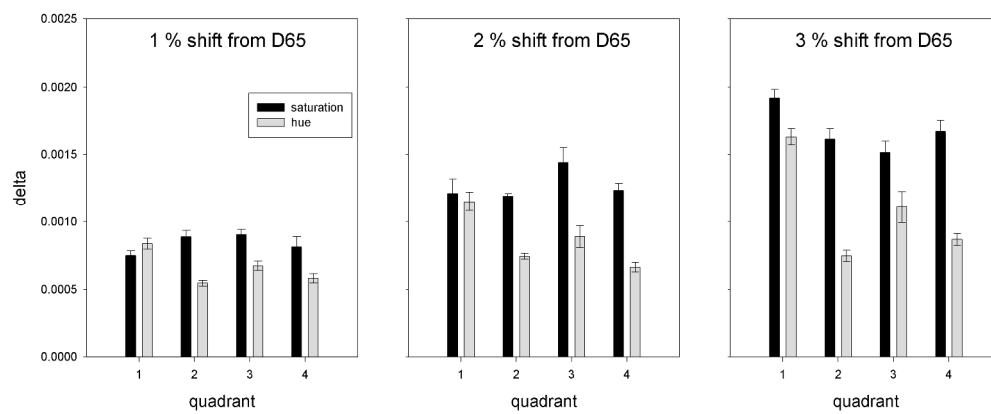
591x246mm (150 x 150 DPI)
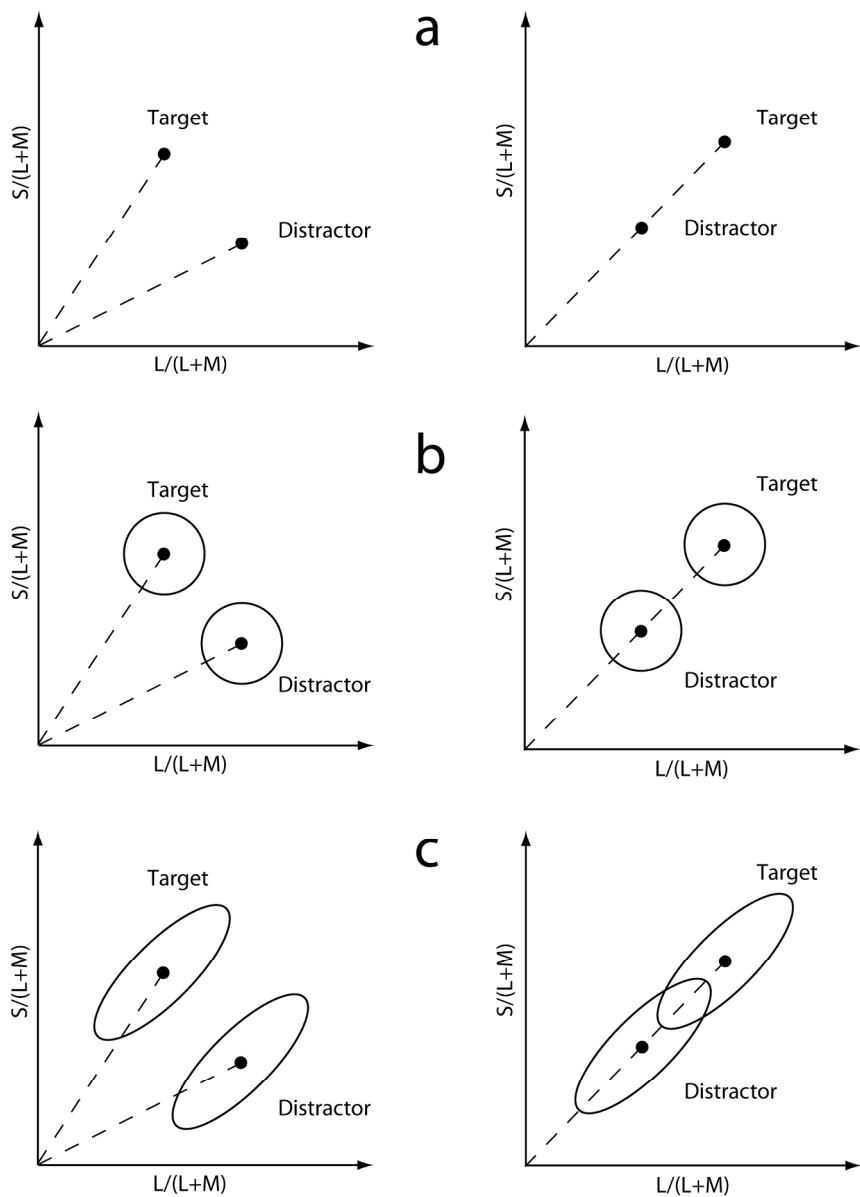
362x362mm (150 x 150 DPI)

251x248mm (150 x 150 DPI)

505x404mm (150 x 150 DPI)

505x404mm (150 x 150 DPI)

159x223mm (300 x 300 DPI)